Entanglement-Enhanced Metrology

Tai Xiang
University of California, Berkeley
(Dated: May 8, 2024)

A statistical derivation through the quantum Fisher information and quantum Cramer-Rao bound yield a $\frac{1}{\sqrt{N}}$ scaling of the uncertainty of an observable with the number of measurements made N given the probe state under measurement is a classical state. However, the use of entanglement can improve this bound to a $\frac{1}{N}$ scaling. One particular probe state of interest is the maximally-entangled N00N state, which can be realized through a multitude of quantum optical techniques. I review some of the methodologies towards achieving high N-valued N00N states and discuss a particular application in photolithography beyond the classical Rayleigh diffraction limit.

I. INTRODUCTION

Advances in precision quantum metrology have yielded insight into a wide variety of new physics and enabled new technologies in areas such as navigation and timekeeping [1, 2]. An especially notable accomplishment is the detection of gravitational waves, ripples in spacetime predicted by Einstein's theory of general relativity, with the Laser Interforemeter Gravitational-Wave Observatory (LIGO). At the heart of these pursuits lies the concept of the standard quantum limit (SQL) and the Heisenberg limit, two fundamental bounds on the precision at which physical quantities can be measured [3, 4]. Beating or saturating these limits not only enhances the precision at which measurements can be performed, but also can also serve as invaluable resources for encoding and processing quantum information with enhanced fidelity and resilience to noise.

During the course, one methodology we discussed was the surpassing of the SQL by the means of squeezed states, quantum states that exhibit reduced uncertainties along certain axes in phase space compared to the vacuum state. Mathematically, squeezing can be characterized by squeezing operators, which act on quantum states to deform their phase space distribution in a manner that selectively reduces uncertainties. Such states were first prosed by Caves [5] and experimentally realized by Grangier et al. [6] and have also seen application in the GEO600 [7] and advanced LIGO detector[8] to surpass the shot noise measurement limit.

In this review, I will cover techniques to surpass the SQL and saturate the Heisenberg limit that do not rely on squeezing, instead leveraging quantum entanglement to achieve so-called superresolution and supersensitivity. I will begin by discussing some basic formalism corresponding to the Standard Quantum Limit and the Heisenberg Limit. I will then review a series of theories and experiments, specifically the proposal and generation of maximally entangled N00N states, that yield measurement results that overcome the SQL. I will conclude by discussing some potential applications in quantum lithography.

II. THE STANDARD QUANTUM LIMIT AND THE HEISENBERG LIMIT

The standard quantum limit is the minimum level of quantum noise that can be obtained when measurements are made on classical systems. There is always some quantum noise present in the system due to the quantum fluctuations stipulated by the Heisenberg uncertainty principle [9].

Statistical errors from such fluctuations can be reduced through repeated measurements, and the ensemble-measurement based method of obtaining expectation values from quantum systems is a method for averaging out such fluctuations in the system. However, the accuracy of these measurements is limited by a scaling resultant from the central limit theorem, which stipulates that n repeated independent measurements each with standard deviation σ, performed on a system will yield a Gaussian distribution with a standard deviation given by

$$\sigma_{ensemble} = \frac{\sigma}{\sqrt{n}}. \tag{1}$$

To more concretely define n, we can consider each measurement to be an instance in which the probe (measurement device) and the system under measurement interact.

It should be noted that this scaling arises purely from classical probability theory and disregards the quantum nature of the probe or the system under measurement. When quantum effects such as entanglement and squeezing are employed, a more advantageous $\frac{1}{n}$ scaling arises, yielding the Heisenberg limit [10].

To better understand the origin of such a bound, let us consider the problem of quantum estimation. Quantum estimation of a continuous parameter x encoded in some state ρ_x of a quantum system S can be given in the following sequence of steps:

1. Perform a measurement on the system S.
2. Process the data obtained from the measurement on S to extrapolate information on the value of x.

Before describing a fully quantum picture of the associated quantum bounds on information, let us first begin with the classical formalism.

A. Classical Statistics

We can define a statistical model $f(x|\theta)$ to be a function that maps a parameter θ to a set of possible measurement outcomes x for some random variable X [11]. A useful metric that dictates the amount of information about θ from a random variable X upon making some number of measurements n is the Fisher information, which is given by

$$I(\theta) = nE_{X;\theta}\left[\left(\partial_\theta \log(f(x|\theta))\right)^2\right] \tag{2}$$

where $E_{X;\theta}$ is the expectation value with respect to $f(x;\theta)$. An alternative form of expression this relation, given that the log likelihood l is twice differentiable, is

$$I(\theta) = -nE_{X;\theta}\left[\partial_\theta^2 \log(f(x|\theta))\right]. \tag{3}$$

The Fisher information can be thought of as a measure of the sensitivity of the statistical model $f(x|\theta)$ when θ changes. The linear relationship with the number of measurement should be noted – an experiment with twenty measurements will be twice as informative as an experiment with ten measurements. A useful construction is the classical Fisher information of the density matrix $\rho(\theta)$, given to be

$$I(\theta) = \sum_b \frac{1}{p(b|\theta)}\partial_\theta^2 p(x|\theta) \tag{4}$$

where $p(b|\theta) = \langle b|\,\rho(\theta)\,|b\rangle$.

An unbiased estimator of a deterministic variable θ has a variance that is bounded by the Cramer-Rao bound, which is defined to be

$$\mathrm{var}(\theta) \geq \frac{1}{I(\theta)}. \tag{5}$$

This condition stipulates that the precision at which θ can be estimated is fundamentally bounded by the Fisher information of the statistical model.

An additional useful metric to analyze is the efficiency of the estimator $e(\theta)$, which describes how close the variance of the estimator is to the Cramer-Rao bound. The efficiency is given to be

$$e(\theta) = \frac{I(\theta)^{-1}}{var(\theta)} \tag{6}$$

and it follows that $e(\theta) \leq 1$. An optimal estimator is one that saturates the Cramer-Rao bound and has an efficiency of 1. Minimizing the uncertainty of parameter estimation can thus be thought of as attempting to maximizing the Fisher information and saturating the Cramer-Rao bound.

III. QUANTUM STATISTICS

Both the Fisher information and the Cramer-Rao bound have quantum analogues, which follow from the Heisenberg uncertainty relation. Let us consider some density matrix ρ given by

$$\rho = \sum_k p_k\,|\psi_k\rangle\,\langle\psi_k|\,. \tag{7}$$

Heisenberg uncertainty dictates that for two operators A and B, we have the following inequality

$$\Delta A^2_{\psi_k}\Delta B^2_{\psi_k} \geq \frac{1}{4}|\langle i[A,B]\rangle_{\psi_k}|^2. \tag{8}$$

For the mixed state, the variance of A can be shown to be

$$(\Delta A)^2_\rho = \sup_{p_k,\psi_k}\sum_k p_k(\Delta A)^2_{\psi_k}. \tag{9}$$

For an estimation parameter θ, we will define its uncertainty to be

$$\Delta\theta^2_A = \frac{\Delta A^2}{|\langle i[A,B]\rangle_{\psi_k}|^2} \tag{10}$$

and upon applying the Cauchy-Schwarz inequality and the above definition 8 of the variance of A, we then see that we have the bound [12]

$$\Delta\theta^2_A = \frac{1}{4\mathrm{max}_{p_k,\psi_k}(\sum_k p_k(\Delta B)^2_{\psi_k})} \tag{11}$$

This is just the quantum Cramer-Rao bound and has the $\frac{1}{\sqrt{n}}$ scaling of the standard quantum limit.

Like the classical analog, the quantum Fisher information is just the term in the denominator, and can be given to be

$$I_Q[\rho,B] = 4\mathrm{max}_{p_k,\psi_k}\left[\sum_k p_k(\Delta B)^2_{\psi_k}\right]. \tag{12}$$

An alternative and perhaps more natural derivation is through the modification of $p(x|\theta)$ with the Born rule and symmetric logarithmic derivative[13]. The Born rule dictates that

$$p(x|\theta) = Tr[\Pi_x\rho_\theta], \tag{13}$$

where Π is a positive operator-valued measure (POVM) and ρ_θ describes the density matrix of the quantity θ we are seeking to measure. A POVM is a map that associates some positive operator with every subset, where the subset includes the possible measurement outcomes and is a more general formalism for describing measurement.

We now define the symmetric logarithmic derivative L_θ, which is given implicitly by

$$i[\rho,\theta] = \frac{1}{2}\{\rho, L_\rho(\theta)\} \tag{14}$$

and explicitly

$$L_\rho(\theta) = 2i \sum_{k,l} \frac{\lambda_k - \lambda_l}{\lambda_k + \lambda_l} \langle k| \theta |l\rangle |k\rangle \langle l| \tag{15}$$

where λ_k and λ_l are the eigenvalues of of the states $|k\rangle$ and $|l\rangle$. With the application of the Born rule and the use of the symmetric logarithmic derivative, the classical Fisher information can then be reconstructed to be

$$F(\theta) = \int dx \frac{Re(Tr[\rho_\theta \Pi_x L_\theta])^2}{Tr[\rho_\theta \Pi_x]}. \tag{16}$$

To obtain a bound to estimation given a quantum system, we must then maximize the classical Fisher information over quantum measurements. This procedure goes as follows:

$$F(\theta) \leq \int dx \left| \frac{Tr[\rho_\theta \Pi_x L_\theta]}{\sqrt{Tr[\rho_\theta \Pi_x]}} \right|^2 \tag{17}$$

$$\leq \int dx Tr[\Pi_x L_\theta \rho_\theta L_\theta] \tag{18}$$

$$= Tr[L_\theta \rho_\theta L_\theta] \tag{19}$$

$$= Tr[\rho_\theta L_\theta^2]. \tag{20}$$

The Quantum Fisher information is thus given to be

$$I_Q(\theta) = Tr[\rho_\theta L_\theta^2] = Tr[\partial_\theta \rho_\theta L_\theta], \tag{21}$$

from which the quantum Cramer-Rao bound then arises:

$$\Delta\theta \geq \frac{1}{\sqrt{nTr[\partial_\theta \rho_\theta L_\theta]}} = \frac{1}{\sqrt{n}} \tag{22}$$

where n once again is the number of measurements [**?**] and we observe a general formulation of the SQL. Physically, such a limit arises from the Poissonian statistics that classical light obeys.

The application of the symmetric logarithmic derivative for the derivation of the quantum Fisher information is important as it yields a method to compute the quantum fisher information for any density matrix. It should be noted that in the large N limit, the quantum Cramer-Rao bound can be provably saturated with local non-quantum enhanced measurement (no entanglement applied during readout or measurement). This implies that surpassing the SQL requires the application of quantum-enhanced techniques during the preparation of the probe [14].

A. Beyond the Standard Quantum Limit

The Quantum Cramer-Rao bound was derived for the case where the set of probe states ρ_θ was fixed and only used to describe the readout stage of the measurement procedure. Additional considerations of the measurement probe preparation as well as the probe-system interaction must be made. As an example, we can consider a system of n entangled probes $\rho_0^{(n)}$. To derive a bound on the precision of measurement, we must optimize with respect to both the entangled probes as well as the overall error with respect to ρ_θ. Performing both optimizations ensures that we will have a precision that is no larger than the quantum Cramer-Rao bound [14], and will thus be of the form

$$\Delta\theta_n \geq \max_{\rho_0^{(n)}} \left[\frac{1}{\sqrt{I_Q}(\rho_\theta)} \right]. \tag{23}$$

The optimal ρ_0 must be a pure state by the convexity of the quantum Fisher information [15]. For a pure state in a closed system that has no loss or decoherence, ρ_0 can be rewritten in terms of the states under measurement ρ_θ. Assuming a unitary measurement protocol denoted by the Hamiltonian H, the input state can be written to be

$$\rho_0 = \rho_x = e^{iH\Theta} H e^{-iH\Theta} \tag{24}$$

which for the case of pure states, enables the quantum Cramer-Rao bound to be written as

$$\Delta\Theta_n \geq \frac{1}{2\Delta H\sqrt{n}}. \tag{25}$$

When the probe states are maximally entangled, we have $2\Delta H = N$, where N is the number of entangled probe states. The resultant scaling then becomes

$$\Delta\Theta_n \geq \frac{1}{\sqrt{nN}} = \frac{1}{N\sqrt{\nu}} \tag{26}$$

where $\nu = nN$ and describes the resource scaling of the system.

To illustrate the resultant $\frac{1}{n}$ Heisenberg scaling, it is perhaps most illuminating to consider the example of Ramsey interferometry, a common technique in atomic, molecular, and optical (AMO) physics. Ramsey interferometry seeks to measure the accumulation of an unknown phase ϕ between two orthogonal states $|0\rangle$ and $|1\rangle$ of an atomic system. An atom prepared in the excited state $|1\rangle$ is hit with a $\pi/2$ pulse, where it is then sent to the superposition state $\frac{1}{\sqrt{2}}(|0\rangle + |1\rangle$. It is allowed to precess and accumulate some phase ϕ, and it eventually enters some state $\frac{1}{\sqrt{2}}(|0\rangle + e^{i\phi}|1\rangle)$. Another $\pi/2$ pulse is then applied, "undoing" the first one, and we find the probability of finding the atom to be in the same final state ψ_f as its initial state ψ_i to be

$$P = |\langle \psi_i | \psi_f \rangle|^2 = \frac{(1 - \cos\phi)}{2} \tag{27}$$

and upon successive measurements, the phase ϕ can then be recovered. For this case, the signal of the measurement is given by $\cos\phi$, whereas the noise is $|\sin\phi$, and for n measurements on n independent atoms, the uncertainty in ϕ is given to be

$$\Delta\phi = \frac{1}{\sqrt{n}} \frac{\sin\phi}{|\frac{d\cos\phi}{d\phi}|} = \frac{1}{\sqrt{n}} \tag{28}$$

which is the bound predicted by the standard quantum limit. We observe that the only scaling is with the number of measurements made, and there is no exploitation of quantum effects to increase measurement precision. However, we can consider an alternative situation in which instead of n independent atoms, we perform this sequence on a maximally entangled GHZ state of n entangled atoms, as described by Bollinger et al. in 1996. For an input state of n atoms $|11\dots11\rangle$, the application of a $\pi/2$ pulse yields the GHZ state $\frac{1}{\sqrt{2}}(|00\dots00\rangle + |11\dots11\rangle)$. Free precession then yields the state $\frac{1}{\sqrt{2}}(|00\dots00\rangle + e^{in\phi}|11\dots11\rangle)$, where we observe a scaling of the accumulated phase with the number of atoms in the input state. Application of the second $\pi/2$ pulse then yields a probability of $P = \frac{1+\cos n\phi}{2}$ and a subsequent standard deviation of

$$\Delta\phi = \frac{1}{n\sqrt{\nu}} \tag{29}$$

where ν is the number of trials performed. By utilizing a maximally entangled input state, we thus observe a scaling of the standard deviation at $\frac{1}{n}$, the so-called Heisenberg limit.

IV. ENTANGLEMENT

A. N00N States

As discussed above, the usage of a highly entangled state as an input to Ramsey interferometry yields an uncertainty on the measurement result that scales as $\frac{1}{n}$, surpassing the standard quantum limit. This methodology has become quite commonplace with photons, to the point where it has received its own special name: The N00N state [16]. Let us consider the case of two sets of entangled photon states A and B going through a Mach-Zehnder Interferometer (MZI), as shown in figure 1. The state A goes through a phase shifter while B does not. This is essentially the same as the aforementioned Ramsey interferometry experiment.

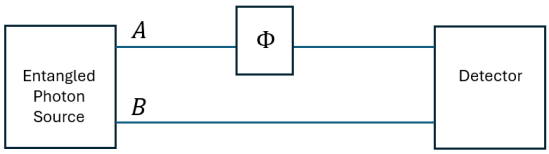

FIG. 1. Entangled photon source emitting two branches A and B. Branch A passes through a phase shifter (ϕ) before reaching the detector.

At the initial output of the photon source, we have a superposition state of N photons in arm A and no photons in arm B and N photons in arm B and no photons in arm A. This is denoted to be

$$|N00N\rangle = \frac{1}{\sqrt{2}}(|N\rangle_A|0\rangle_B + |0\rangle_A|N\rangle_B). \tag{30}$$

When a number state enters a phase shifter, it evolves in accordance with the unitary operator

$$U(\phi) = e^{-iN\phi} \tag{31}$$

and thus the resultant output at the detectors is given by

$$|N00N\rangle = \frac{1}{\sqrt{2}}(|N\rangle_A|0\rangle_B + e^{-iN\phi}|0\rangle_A|N\rangle_B). \tag{32}$$

The measurement result on each photodetector is given by

$$I_{MA} = I_A \sin^2(\phi/2) \tag{33}$$

$$I_{MB} = I_B \cos^2(\phi/2) \tag{34}$$

where I denotes the intensity of the incident light. The subtracted signal is then

$$M(\phi) = I_{MA} - I_{MB} = I_A \cos\phi \tag{35}$$

Such a measurement corresponds to the observable M, given by

$$M = |N\rangle|0\rangle\langle 0|\langle N| + |0\rangle|N\rangle\langle N|\langle 0| \tag{36}$$

and the uncertainty in θ is thus given by

$$\Delta\theta = \frac{\Delta A}{|d\langle A\rangle/d\theta|} = 1/N \tag{37}$$

where we observe the Heisenberg scaling.

B. Generation of N00N States

Low photon number N00N states are fairly straightforwards to generate. First, a single photon undergoes spontaneous parametric down-conversion (SPDC) where it becomes a pair of number states. Passage through a beamsplitter then yields the state

$$|\psi\rangle = \frac{1}{\sqrt{2}}(|2\rangle_A|0\rangle_B + |0\rangle_A|2\rangle_B \tag{38}$$

as stipulated by the Hong-Ou-Mandel (HOM) effect (cross terms cancel due to destructive interference) [9].

Though not fully exploiting the lower uncertainty that arises for higher values of N, the demonstration of the $1/n$ scaling in experiments applying two-photon states is still a topic of high interest. Zhou et al. performed demonstrated a super-resolving phase measurement with N00N states in 2017 [17]. They up-converted a photon pair from 1547 nm to 525 nm type 1 periodically poled potassium crystal before sending the state through

a beamsplitter and then through detectors, in a similar set-up to the one draw in figure 1. The purpose of this up-conversion was to increase the sensitivity of optical path length measurements and also reduce diffraction effects during imaging, as such effects scale with the wavelength. To validate the fidelity of their state generation, Zhou et al. performed a HOM experiment and observe nearly perfect $(96.72 \pm 0.82\%)$ interference between the generated 525 nm photon pair.

The two-photon N00N state is then sent to a Sagnac interferometer, where the two-photon interference fringe is measured with a visibility of $84.93 \pm 3.18\%$, surpassing the standard quantum limit visibility threshold of 71%. This result is shown in figure 3. The visibility is defined

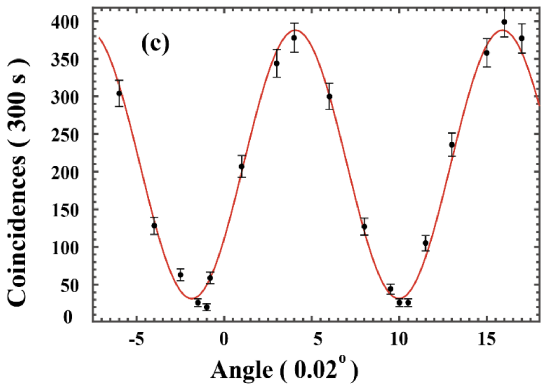

FIG. 2. Interference pattern of the two-photon N00N state as a function of the rotation angle of the phase plate, which is used to induce the phase shift ϕ. Figure taken from Zhou et al..

to be the ratio of the amplitude of the interference pattern to the sum of the powers of the input signals, or

$$v = \frac{2\sqrt{I_1 I_2}\phi}{I_1 + I_2}. \tag{39}$$

There has also been attention to the shrinking of the architecture required to generate such states so as to make them more applicable and scalable for creating Heisenberg limited sensing networks. Verma et al. proposed a methodology that involved the usage of a quantum dot embedded in a crystal microcavity [18], while Vergyris et al. successfully demonstrated the heralded generation of a two-photon N00N state on a chip with the use of nonlinear wave-guides and femtosecond lasers [19]. This realization achieved a two-photon visibility of $90 \pm 8\%$ and a fidelity of $95 \pm 8\%$, with a rather high loss of 14dB.

Achieving higher N-valued N00N states is a non-trivial procedure. Let us first examine a similar SPDC procedure. For a strong pump, SPDC produces un-entangled number states (twin-Fock states) of form

$$|\psi\rangle = |N/2\rangle_A |N/2\rangle_B \tag{40}$$

in modes A and B. However, the input of these twin states at the input of a beamsplitter does not immediately yield a high N-valued N00N state (high N00N), as the generalized HOM effect [20] yields the following output state:

$$|N/2\rangle_A |N/2\rangle_B \xrightarrow{\text{BS}} \tag{41}$$
$$c_N |N\rangle_C |0\rangle_D + c_{N-2} |N-2\rangle_C |2\rangle_D + \tag{42}$$
$$\cdots + c_{N-2} |2\rangle_C |N-2\rangle_D + c_N |0\rangle_C |N\rangle_D \tag{43}$$

where C and D are the output modes of the beamsplitter and c_N are amplitude weight factors for each state. We observe the desired high N states on the outer edges of the beamsplitter output, but there is a large quantity of crossterms in the middle that we wish to get rid of. Thus, to achieve a high N00N state, some technique must be implemented to remove the middle portion.

One such proposal was made by Gerry and Campos in 2002 [21], employing two MZIs coupled by a cross-Kerr phase shifter and a quantum-optical Fredkin gate. The implementation of a Fredkin gate (a controlled-swap gate), as shown in figure **??** enables a single photon in the first MZI to control the phase shift in the second MZI.

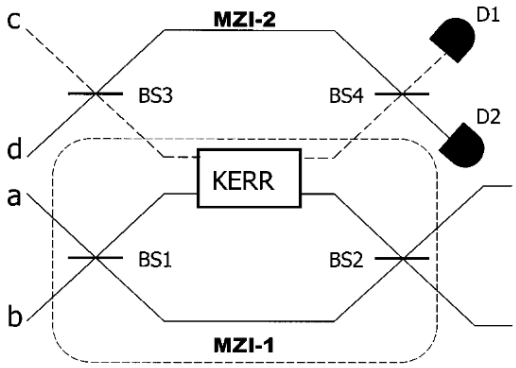

FIG. 3. Schematic of an optical Fredkin gate that implements a controlled swap with two MZIs and a cross-Kerr medium. Figure taken from Gerry and Campos.

The output state of such a system is

$$|\psi\rangle_{out} = \frac{1}{2}[(|N\rangle_a |0\rangle_b + e^{-iN\pi/2} |0\rangle_a |N\rangle_b) |1\rangle_c |0\rangle_d \tag{44}$$
$$+ i(|N\rangle_a |0\rangle_b + e^{-iN\pi/2} |0\rangle_a |N\rangle_b) |0\rangle_c |1\rangle_d] \tag{45}$$

for which the Heisenberg limit can be saturated.

Though such a methodology appears to resolve the issue of high N00N state generation, it is heavily limited by the efficiency of the nonlinear Kerr medium. For $N = 10$, the system would yield a phase shift of $10^{-20}\pi$ [22]. One substitution for this nonlinear Kerr medium is to apply the efficiency quantum computing with linear optics paradigm introduced by Knill et al. in 2001 [23]. In such a scheme, an effective Kerr nonlinearity can be achieved through a combination of mirrors, phase

shifters, beamsplitters, and detectors at a far higher efficiency. Lee et al. proposed a method of high N00N state generation with the aforementioned methodology, utilizing solely linear optical components [24] as shown in figure 4. They claim that this set-up can achieve a four photon N00N state. Post-selection on one photon being

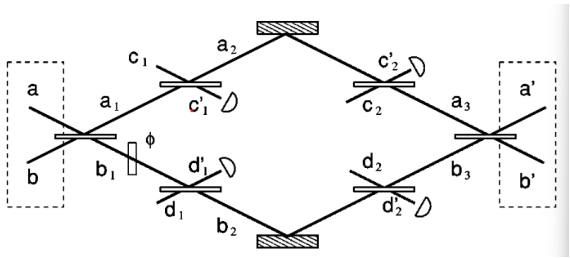

FIG. 4. A four-detector MZI interferometer that utilizes measurement-based conditioning to realize a high N00N state. Figure taken from Lee et al.

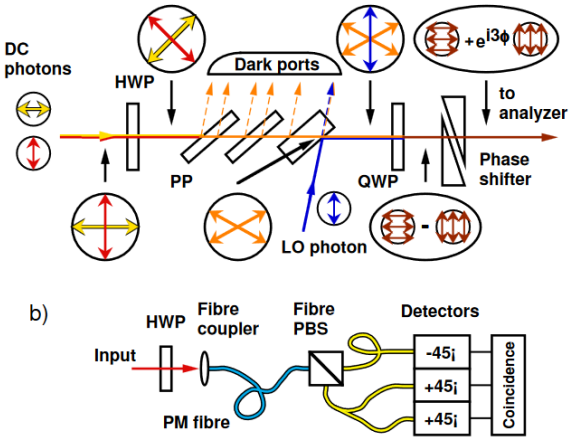

FIG. 5. a) demonstrates the sequence of optical components that condition the polarization of the input photons. b) demonstrates the detector set-up that realizes the post-selection protocol.

measured at each detector yields the desired high N00N state without the need for nonlinear optical elements and boost the efficiency to 10^{-1} However, this post-selection protocol scales exponentially with N, meaning that the likelihood of getting a N00N state is exponentially decreases for a larger input state. This scheme can then be stacked to realize arbitrarily high N N00N states [25].

Efforts to improve the exponential decay of efficiency with N in the linear optics scheme have been made [26, 27], while other techniques that seek to circumvent the linear optics formalism have also been explored [28]. Presently, experimentally realizing such states are still quite challenging.

C. Experimental Realizations of High N00N States

In 2003, Mitchell et al. experimentally realized a three-photon N00N state [29] with a postselection scheme shown in figure 5 with an success rate of 72%. In their experiment, two photons from from pulsed parametric down-conversion and another local oscillator photon generated from a laser. The down-converted photons are orthogonally polarized, and upon polarization conditioning, post-selection for cases of no photon reflection off the polarization beam splitter shown in figure 5 confirm the creation of a N00N state.

A four-photon N00N state in a similar linear optics post-selection scheme was realized by Walther et al. in 2004 with the experimental apparatus shown in figure 6. Spontaneous parametric down-conversion of the pump beam produces a pair of energy-degenerate polarization-entangled photons. The pump beam is then reflected and emits another pair of photons into a different set of modes, and a methodology analogous to the proposal by Lee et al. was applied to attain the desired output four-photon N00N state.

In 2008, Higgins et al. realized an alternative method

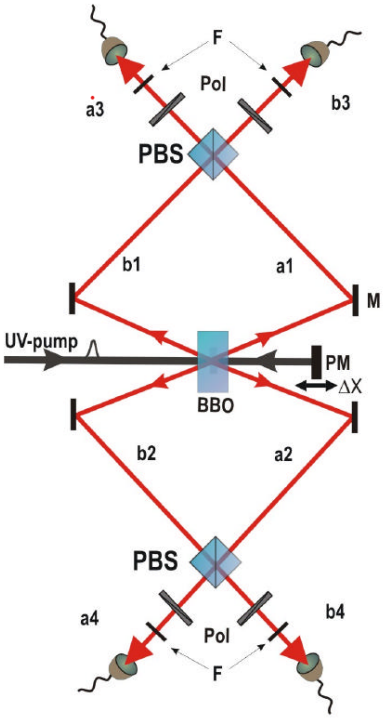

FIG. 6. The four-photon N00N state preparation apparatus. a_1, a_2, b_1, and b_2 denote the output modes of the photons emitted through spontaneous parametric down-conversion through the BBO crystal. A pump mirror PM is position-scanned by a piezo to tune the phases between the two pairs of photons.

that enabled phase estimation up to the Heisenberg limit, though the state realized by this procedure is not entirely identical high N N00N state. Instead, they input a $N = 1$

N00N state through an interferometer 378 times, applying feedback at each pass to realize N entangled single-photon states. This protocol is effectively equivalent to applying a generalization of Kitaev's phase estimation algorithm and can circumvent the high detector overhead for realizing a complicated N00N state at the cost of additional electronics and feedback mechanisms. Though not a traditional N00N state, Higgins et al. similarly demonstrate a Heisenberg-like scaling of phase estimation, as shown in figure 7.

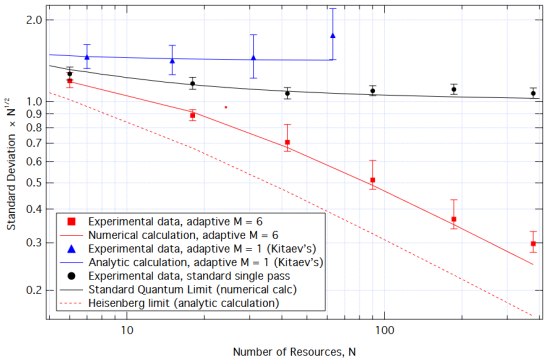

FIG. 7. Comparisons of experimental data with theoretical scaling laws for the system under measurement. It is clearly seen that the algorithm realized by Higgins et al. (red squares) surpassed the SQL and has a Heisenberg like behavior.

V. APPLICATIONS

There are a handful of potential application for the aforementioned Heisenberg-scaling N00N states, such as quantum coherence tomography [30], quantum remote sensing for laser interferometric radar, the miniturization of sensors [31], quantum information and communication [32], and even extensions to chemistry and biology [33]. I will focus on quantum lithography.

Quantum lithography is a sub-area of quantum imaging that leverages the uncertainty scaling of N00N states to surpass the Rayleigh diffraction limit for the purpose of photolithography. Photolithography is a procedure that is commonplace in the manufacturing of integrated circuits, and utilizes photons to etch patterns in a photoabsorptive material (photoresist) down to the nanometer scale. Complex patterns can be etched to realize complex integrated circuits, including solid state memories and microprocessors [34].

In photolithography and related manufacturing processes, there exists a minimally resolveable distance that is given by

$$\Delta x = \lambda \tag{46}$$

where λ is the wavelength of the incident light on the photo-absorptive material. This Rayleigh diffraction limit yields a restriction on how far components can be placed next to one another. For example, when performing etching with a 420 nm light, one cannot place two components less than 420 nm apart, greatly bounding how small components can be fabricated.

N00N states can provide superresolution for lithographic procedures. This effect can be understood by drawing equivalence to an N-photon absorption and an N-photon detection process. For a N00N state, the number of photons detected is

$$\bar{n}(\theta) = \langle N00N| \, (a^\dagger)^N (a)^N \, |N00N\rangle \tag{47}$$
$$= 1 + \cos(N\theta) \tag{48}$$

and for an MZI, $\theta = kx = \frac{2\pi x}{\lambda}$ where x describes the displacements between the two arms of the interferometer. When compared with the photolithographic resolution when no entanglement is applied to the state under measurement, we find that

$$\lambda_{N00N} = \lambda_{classical}/N, \tag{49}$$

enabling etching at scales that go beyond the diffraction limit. Such a method is not only useful for superresolution, but can also yield large cost savings. Due to the wavelength scaling of position uncertainty, lithographic companies seek to push etching wavelengths to the X-ray range [35]. However, moving to these wavelengths requires adapting all other imaging systems to these lower wavelengths, and thus the cheaper technology and hardware for optical wavelengths is no longer useable. However, photoetching with N00N states at an optical wavelength would yield the same gains on positional uncertainty as photoetching in the X-ray range while still preserving the low-cost and pre-existing accompaniments that are required in the procedure. A small demonstration of this proposal was realized by Chang et al. with polymethyl-methacrylate, a UV lithographic material that is excited by multi-photon absorption in the visible region [36]. Using a 800nm titanium sapphire laser as the etching tool, Chang et al. were able to resolve etching fringes at a period of around 213 nm, thus overcoming the classical Rayleigh diffraction limit. Atomic force microscopy of their etched samples are shown in figure 8.

However, while this proposal sounds straightforwards and experimental demonstrations seem effective, a challenge for realizing the full potential of N00N state-enhanced lithography is that N-photon absorbing resists are generally impractical for quantum lithography. Typical lithographic materials are optimized for single photon absorption, whereas to attain the full benefit of high N00N states, materials would need to be able to tolerate absorption of a large number of photons [16]. Advancements in chemistry are likely required to formulate a lithographic material that can fully utilize the power of N00N states.

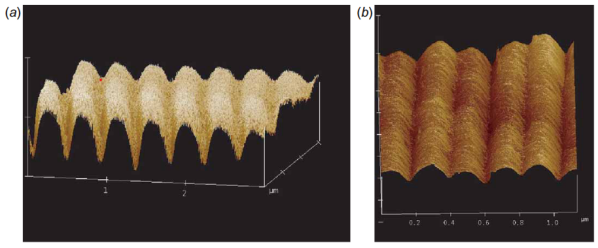

FIG. 8. Atomic force microscopy images of the fringes recorded on the etched poly-methacrylate lithographic material. (a) corresponds to a single exposure with fringes of 425 nm in periodicity while (b) corresponds to a two-exposure sequence with a periodicity of 213 nm.

[1] Lin Jiao, Wei Wu, Si-Yuan Bai, and Jun-Hong An. Quantum metrology in the noisy intermediate-scale quantum era. *Advanced Quantum Technologies*, November 2023.

[2] Andrew D. Ludlow, Martin M. Boyd, Jun Ye, Ekkehard Peik, and Piet O. Schmidt. Optical atomic clocks, 2015.

[3] Torrey Cullen, Ron Pagano, Jonathan Cripe, Safura Sharifi, Michelle Lollie, Scott Aronson, Henry Cain, Paula Heu, David Follman, Garrett D Cole, Nancy Aggarwal, and Thomas Corbitt. Surpassing the standard quantum limit using an optical spring, 2022.

[4] Zain H. Saleem, Michael Perlin, Anil Shaji, and Stephen K. Gray. Achieving the heisenberg limit with dicke states in noisy quantum metrology, 2024.

[5] Carlton M. Caves. Quantum-mechanical noise in an interferometer. *Phys. Rev. D*, 23:1693–1708, Apr 1981.

[6] P. Grangier, R. E. Slusher, B. Yurke, and A. LaPorta. Squeezed-light–enhanced polarization interferometer. *Phys. Rev. Lett.*, 59:2153–2156, Nov 1987.

[7] A gravitational wave observatory operating beyond the quantum shot-noise limit. *Nature Physics*, 7(12):962–965, September 2011.

[8] F. Acernese, M. Agathos, L. Aiello, A. Allocca, A. Amato, S. Ansoldi, S. Antier, M. Arène, N. Arnaud, S. Ascenzi, P. Astone, F. Aubin, S. Babak, P. Bacon, F. Badaracco, M. K. M. Bader, J. Baird, F. Baldaccini, G. Ballardin, G. Baltus, C. Barbieri, P. Barneo, F. Barone, M. Barsuglia, D. Barta, A. Basti, M. Bawaj, M. Bazzan, M. Bejger, I. Belahcene, S. Bernuzzi, D. Bersanetti, A. Bertolini, M. Bischi, M. Bitossi, M. A. Bizouard, F. Bobba, M. Boer, G. Bogaert, F. Bondu, R. Bonnand, B. A. Boom, V. Boschi, Y. Bouffanais, A. Bozzi, C. Bradaschia, M. Branchesi, M. Breschi, T. Briant, F. Brighenti, A. Brillet, J. Brooks, G. Bruno, T. Bulik, H. J. Bulten, D. Buskulic, G. Cagnoli, E. Calloni, M. Canepa, G. Carapella, F. Carbognani, G. Carullo, J. Casanueva Diaz, C. Casentini, J. Castañeda, S. Caudill, F. Cavalier, R. Cavalieri, G. Cella, P. Cerdá-Durán, E. Cesarini, O. Chaibi, E. Chassande-Mottin, F. Chiadini, R. Chierici, A. Chincarini, A. Chiummo, N. Christensen, S. Chua, G. Ciani, P. Ciecielag, M. Cieślar, R. Ciolfi, F. Cipriano, A. Cirone, S. Clesse, F. Cleva, E. Coccia, P.-F. Cohadon, D. Cohen, M. Colpi, L. Conti, I. Cordero-Carrión, S. Corezzi, D. Corre, S. Cortese, J.-P. Coulon, M. Croquette, J.-R. Cudell, E. Cuoco, M. Curylo, B. D'Angelo, S. D'Antonio, V. Dattilo, M. Davier, J. Degallaix, M. De Laurentis, S. Deléglise, W. Del Pozzo, R. De Pietri, R. De Rosa, C. De Rossi, T. Dietrich, L. Di Fiore, C. Di Giorgio, F. Di Giovanni, M. Di Giovanni, T. Di Girolamo, A. Di Lieto, S. Di Pace, I. Di Palma, F. Di Renzo, M. Drago, J.-G. Ducoin, O. Durante, D. D'Urso, M. Eisenmann, L. Errico, D. Estevez, V. Fafone, S. Farinon, F. Feng, E. Fenyvesi, I. Ferrante, F. Fidecaro, I. Fiori, D. Fiorucci, R. Fittipaldi, V. Fiumara, R. Flaminio, J. A. Font, J.-D. Fournier, S. Frasca, F. Frasconi, V. Frey, G. Fronzè, F. Garufi, G. Gemme, E. Genin, A. Gennai, Archisman Ghosh, B. Giacomazzo, M. Gosselin, R. Gouaty, A. Grado, M. Granata, G. Greco, G. Grignani, A. Grimaldi, S. J. Grimm, P. Gruning, G. M. Guidi, G. Guixé, Y. Guo, P. Gupta, O. Halim, T. Harder, J. Harms, A. Heidmann, H. Heitmann, P. Hello, G. Hemming, E. Hennes, T. Hinderer, D. Hofman, D. Huet, V. Hui, B. Idzkowski, A. Iess, G. Intini, J.-M. Isac, T. Jacqmin, P. Jaranowski, R. J. G. Jonker, S. Katsanevas, F. Kéfélian, I. Khan, N. Khetan, G. Koekoek, S. Koley, A. Królak, A. Kutynia, D. Laghi, A. Lamberts, I. La Rosa, A. Lartaux-Vollard, C. Lazzaro, P. Leaci, N. Leroy, N. Letendre, F. Linde, M. Llorens-Monteagudo, A. Longo, M. Lorenzini, V. Loriette, G. Losurdo, D. Lumaca, A. Macquet, E. Majorana, I. Maksimovic, N. Man, V. Mangano, M. Mantovani, M. Mapelli, F. Marchesoni, F. Marion, A. Marquina, S. Marsat, F. Martelli, V. Martinez, A. Masserot, S. Mastrogiovanni, E. Mejuto Villa, L. Mereni, M. Merzougui, R. Metzdorff, A. Miani, C. Michel, L. Milano, A. Miller, E. Milotti, O. Minazzoli, Y. Minenkov, M. Montani, F. Morawski, B. Mours, F. Muciaccia, A. Nagar, I. Nardecchia, L. Naticchioni, J. Neilson, G. Nelemans, C. Nguyen, D. Nichols, S. Nissanke, F. Nocera, G. Oganesyan, C. Olivetto, G. Pagano, G. Pagliaroli, C. Palomba, P. T. H. Pang, F. Pannarale, F. Paoletti, A. Paoli, D. Pascucci, A. Pasqualetti, R. Passaquieti, D. Passuello, B. Patricelli, A. Perego, M. Pegoraro, C. Périgois, A. Perreca, S. Perriès, K. S. Phukon, O. J. Piccinni, M. Pichot, M. Piendibene, F. Piergiovanni, V. Pierro, G. Pillant, L. Pinard, I. M. Pinto, K. Piotrzkowski, W. Plastino, R. Poggiani, P. Popolizio, E. K. Porter, M. Prevedelli, M. Principe, G. A. Prodi,

M. Punturo, P. Puppo, G. Raaijmakers, N. Radulesco, P. Rapagnani, M. Razzano, T. Regimbau, L. Rei, P. Rettegno, F. Ricci, G. Riemenschneider, F. Robinet, A. Rocchi, L. Rolland, M. Romanelli, R. Romano, D. Rosińska, P. Ruggi, O. S. Salafia, L. Salconi, A. Samajdar, N. Sanchis-Gual, E. Santos, B. Sassolas, O. Sauter, S. Sayah, D. Sentenac, V. Sequino, A. Sharma, M. Sieniawska, N. Singh, A. Singhal, V. Sipala, V. Sordini, F. Sorrentino, M. Spera, C. Stachie, D. A. Steer, G. Stratta, A. Sur, B. L. Swinkels, M. Tacca, A. J. Tanasijczuk, E. N. Tapia San Martin, S. Tiwari, M. Tonelli, A. Torres-Forné, I. Tosta e Melo, F. Travasso, M. C. Tringali, A. Trovato, K. W. Tsang, M. Turconi, M. Valentini, N. van Bakel, M. van Beuzekom, J. F. J. van den Brand, C. Van Den Broeck, L. van der Schaaf, M. Vardaro, M. Vasúth, G. Vedovato, D. Verkindt, F. Vetrano, A. Viceré, J.-Y. Vinet, H. Vocca, R. Walet, M. Was, A. Zadrożny, T. Zelenova, J.-P. Zendri, Henning Vahlbruch, Moritz Mehmet, Harald Lück, and Karsten Danzmann. Increasing the astrophysical reach of the advanced virgo detector via the application of squeezed vacuum states of light. *Phys. Rev. Lett.*, 123:231108, Dec 2019.

[9] Christopher Gerry and Peter Knight. *Introductory Quantum Optics*. Cambridge University Press, 2004.

[10] Vittorio Giovannetti, Seth Lloyd, and Lorenzo Maccone. Advances in quantum metrology. *Nature Photonics*, 5(4):222–229, Apr 2011.

[11] L. Savage. *The Foundations of Statistics*. Dover, 1954.

[12] Sergio Boixo, Steven T. Flammia, Carlton M. Caves, and JM Geremia. Generalized limits for single-parameter quantum estimation. *Phys. Rev. Lett.*, 98:090401, Feb 2007.

[13] Matteo G. A. Paris. Quantum estimation for quantum technology, 2009.

[14] Vittorio Giovannetti, Seth Lloyd, and Lorenzo Maccone. Quantum-enhanced measurements: Beating the standard quantum limit. *Science*, 306(5700):1330–1336, 2004.

[15] S. Alipour and A. T. Rezakhani. Extended convexity of quantum fisher information in quantum metrology. *Physical Review A*, 91(4), April 2015.

[16] Jonathan P. Dowling. Quantum optical metrology–the lowdown on high-n00n states. *Contemporary Physics*, 49(2):125–143, March 2008.

[17] Zhi-Yuan Zhou, Shi-Long Liu, Shi-Kai Liu, Yin-Hai Li, Dong-Sheng Ding, Guang-Can Guo, and Bao-Sen Shi. Superresolving phase measurement with short-wavelength noon states by quantum frequency up-conversion. *Phys. Rev. Appl.*, 7:064025, Jun 2017.

[18] J. K. Verma, Harmanpreet Singh, and P. K. Pathak. Generation of two-photon noon state and polarization-entangled state from a single quantum dot embedded inside a microcavity. *J. Opt. Soc. Am. B*, 36(5):1200–1207, May 2019.

[19] Panagiotis Vergyris, Thomas Meany, Tommaso Lunghi, Gregory Sauder, James Downes, M. J. Steel, Michael J. Withford, Olivier Alibart, and Sébastien Tanzilli. On-chip generation of heralded photon-number states. *Scientific Reports*, 6(1), October 2016.

[20] Yuan Liang Lim and Almut Beige. Generalized hong–ou–mandel experiments with bosons and fermions. *New Journal of Physics*, 7:155–155, July 2005.

[21] Christopher C. Gerry and R. A. Campos. Generation of maximally entangled photonic states with a quantum-optical fredkin gate. *Phys. Rev. A*, 64:063814, Nov 2001.

[22] Pieter Kok, Samuel L Braunstein, and Jonathan P Dowling. Quantum lithography, entanglement and heisenberg-limited parameter estimation. *Journal of Optics B: Quantum and Semiclassical Optics*, 6(8):S811–S815, July 2004.

[23] E. Knill, R. Laflamme, and G. J. Milburn. A scheme for efficient quantum computation with linear optics. *Nature*, 409(6816):46–52, Jan 2001.

[24] Hwang Lee, Pieter Kok, Nicolas J. Cerf, and Jonathan P. Dowling. Linear optics and projective measurements alone suffice to create large-photon-number path entanglement. *Phys. Rev. A*, 65:030101, Mar 2002.

[25] Pieter Kok, Hwang Lee, and Jonathan P. Dowling. Creation of large-photon-number path entanglement conditioned on photodetection. *Phys. Rev. A*, 65:052104, Apr 2002.

[26] N. M. VanMeter, P. Lougovski, D. B. Uskov, K. Kieling, J. Eisert, and Jonathan P. Dowling. General linear-optical quantum state generation scheme: Applications to maximally path-entangled states. *Phys. Rev. A*, 76:063808, Dec 2007.

[27] Kishore T. Kapale and Jonathan P. Dowling. Bootstrapping approach for generating maximally path-entangled photon states. *Phys. Rev. Lett.*, 99:053602, Aug 2007.

[28] Lu Zhang and Kam Wai Clifford Chan. Efficient methods for generating multi-mode noon states. *Optics Communications*, 452:258–263, 2019.

[29] M. W. Mitchell, J. S. Lundeen, and A. M. Steinberg. Super-resolving phase measurements with a multiphoton entangled state. *Nature*, 429(6988):161–164, May 2004.

[30] Magued B. Nasr, Bahaa E. A. Saleh, Alexander V. Sergienko, and Malvin C. Teich. Demonstration of dispersion-canceled quantum-optical coherence tomography. *Phys. Rev. Lett.*, 91:083601, Aug 2003.

[31] Kishore T. Kapale, Leo D. Didomenico, Hwang Lee, Pieter Kok, and Jonathan P. Dowling. Quantum interferometric sensors, 2005.

[32] Jian-Wei Pan, Zeng-Bing Chen, Chao-Yang Lu, Harald Weinfurter, Anton Zeilinger, and Marek Żukowski. Multiphoton entanglement and interferometry. *Rev. Mod. Phys.*, 84:777–838, May 2012.

[33] J. Haas, M. Schwartz, U. Rengstl, M. Jetter, P. Michler, and B. Mizaikoff. Chem/bio sensing with non-classical light and integrated photonics. *Analyst*, 143:593–605, 2018.

[34] H. Tanaka. *Handbook of Crystal Growth: Thin Films and Epitaxy*. Elsevier, 2015.

[35] Amardeep Bharti, Alessio Turchet, and Benedetta Marmiroli. X-ray lithography for nanofabrication: Is there a future? *Frontiers in Nanotechnology*, 4, 2022.

[36] Malcolm N. O'Sullivan-Hale Hye Jeong Chang, Heedeuk Shin and Robert W. Boyd. Implementation of sub-rayleigh-resolution lithography using an n -photon absorber. *Journal of Modern Optics*, 53(16-17):2271–2277, 2006.